Drag Coefficients at Low Reynolds Numbers For Flow Past Immersed Bodies

A. M. JONES and J. G. KNUDSEN

Oregon State College, Corvallis, Oregon

Drag coefficients were determined at low Reynolds numbers for cylinders ($0.1 \leq Re \leq 1.0$) and flat plates ($0.05 \leq Re \leq 2.0$) moving through a viscous medium. The drag coefficient was calculated from the force required to move the immersed body through the fluid, and preliminary work on spheres was used to calibrate the apparatus. For all bodies studied the drag coefficient was inversely proportional to the Reynolds number. The data were analyzed by a least-squares method to obtain the relationship between drag coefficient and Reynolds number.

The diameter of the tank containing the viscous fluid had a very definite effect upon the drag coefficient of the various cylinders and flat plates studied. In the range of D_T/D (tank diameter/cylinder diameter) studied the relationships recommended by White involving the wall effect and the end correction agree with experimental data for values of L/D (cylinder length/cylinder diameter) greater than 16. At L/D ratios less than this drag coefficients are lower than those predicted by White's equations, and the experimental curves are recommended for these ratios.

For flat plates in perpendicular flow no effect of the W/L (plate width/plate length) was detected in the range studied. The tank diameter however had a considerable effect, and a curve is proposed to predict drag coefficients for flat plates in perpendicular flow in the range of experimental conditions studied.

Laminar flow at very low Reynolds numbers over immersed bodies is important in many engineering problems. In aerodynamics it is important in high altitude flight of aircraft. Other problems include lubrication and flow of heavy oils over banks of tubes. Many polymers are highly viscous materials, and in mixing these the power requirement is a function of the force required to move the agitator through the viscous medium.

At present there are several theoretical solutions for predicting drag coefficients for flow over spheres, cylinders, and flat plates in the range of Reynolds numbers from 0.01 to 10. Little experimental data exist however.

The drag force exerted on a body as a fluid moves past it is related to the geometry of the immersed body and the properties of the fluid by a nondimensional drag coefficient which is defined by

$$f_D = \frac{2g_c F}{A_p \rho U^2} \qquad (1)$$

The drag coefficient is a function of the Reynolds number LU/ν for geometrically similar bodies. If geometric similarity does not exist, various length ratios must also affect the drag coefficient.

The present investigation involved determination of the drag coefficient as a function of Reynolds number and various geometric ratios for spheres, cylinders, and flat plates at Reynolds numbers ranging from 0.01 to 1.0. Drag coefficients were determined by measuring the force required to move the body through a viscous fluid and calculating the drag coefficient by use of Equation (1).

THEORY

The laminar motion of viscous incompressible fluids is governed by the Navier-Stokes equation and the continuity equation. For given boundary conditions a solution of these equations gives the velocity and pressure field in a fluid. Local and total drag coefficients may be calculated from this solution by calculating the shear stress at the solid boundaries of the system.

In 1850 Stokes (*13*) published the well-known solution for a sphere moving in an infinite fluid. This solution gives the force of resistance as

$$F = \frac{6\pi\mu U r}{g_c} \qquad (2)$$

Combining Equation (2) with Equation (1) one gets

$$f_D = 24/N_{Re} \qquad (3)$$

where

$$N_{Re} = DU/\nu \qquad (4)$$

Equation (3) holds for Reynolds numbers up to 1.0. Oseen (*11*) linearized the Navier-Stokes equations and obtained the following expression for drag coefficients of spheres:

$$f_D = \frac{24}{N_{Re}}\left(1 + \frac{3}{16}N_{Re}\right) \qquad (5)$$

Equation (5) is suitable for Reynolds numbers up to 5. Goldstein (*4*) solved Oseen's equations, taking into account the higher power terms in the series solutions that were omitted by Oseen. This solution covers Reynolds numbers up to 10.

Experimental data on spheres have been obtained by Liebster (*10*) in the Reynolds number range 0.1 to 10. His results are in agreement with those of Stokes, Oseen, and Goldstein in their respective Reynolds number ranges.

Drag coefficients at low Reynolds numbers for flow of an infinite fluid past infinite circular cylinders have been calculated by Lamb (9), who obtained the following solution:

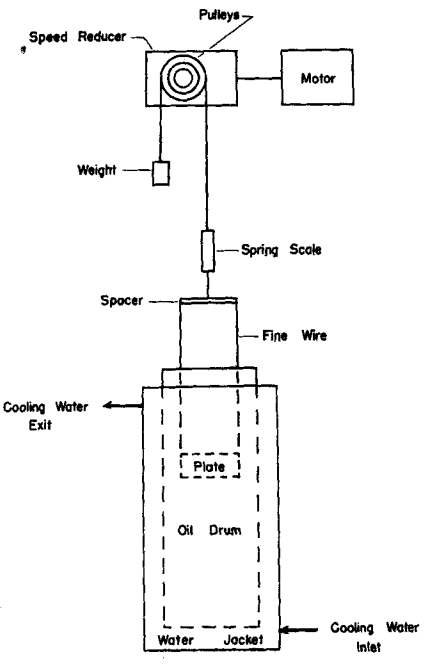

Fig. 1. Block diagram of apparatus.

A. M. Jones is at Yale University, New Haven, Connecticut.

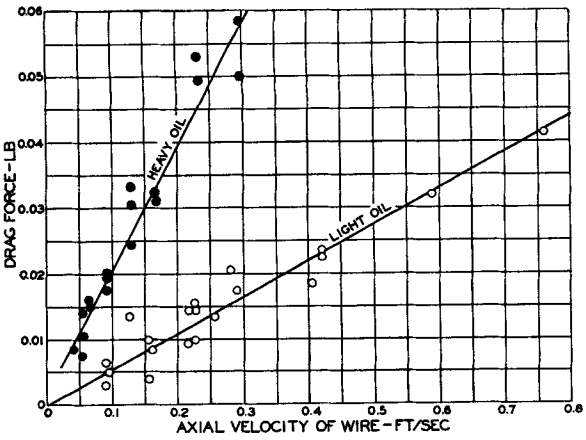

Fig. 2. Drag force on 0.003-in. diameter moving axially out of the oil.

$$f_D = \frac{8\pi}{N_{Re}(2.002 - \ln(N_{Re})} \qquad (6)$$

This solution agrees with experimental data up to a Reynolds number of 0.5.

Bairstow, Cave, and Lang (2) extended Lamb's solution and obtained results which agreed with experimental data up to a Reynolds number of 1.0.

In recent years several investigators have developed approximate solutions of drag coefficients for flow at a low Reynolds number over infinite elliptic cylinders for various ratios of major and minor axes and angles of incidence. For the major axis equal to the minor axis the result is applicable to circular cylinders. For a ratio of major axis to minor axis of infinity the result is a flat plate in parallel flow for a zero angle of incidence and a flat plate in perpendicular flow for an angle of incidence of 90 deg.

Tomotika and Aoi (*15*) obtained exact numerical solutions of Oseen's equations for steady flow past elliptic cylinders of infinite span. Their results, summarized in the following equations, are generally applicable up to a Reynolds number of 1.0.

1. Flat plate in parallel flow

$$f_D = \frac{4\pi}{N_{Re}S}$$

$$\left[1 - \frac{1}{S}\left(S^2 - S - \frac{5}{12}\right)\frac{N_{Re}^2}{128}\right] \qquad (7)$$

$$S = 3.1954 - \ln N_{Re}$$

2. Flat plate in perpendicular flow

$$f_D = \frac{8\pi}{N_{Re}S}$$

$$\left[1 - \frac{1}{S}\left(S^2 + S + \frac{1}{4}\right)\frac{N_{Re}^2}{128}\right] \qquad (8)$$

$$S = 2.1954 - \ln N_{Re}$$

3. Circular cylinder

$$f_D = \frac{9\pi}{N_{Re}S}$$

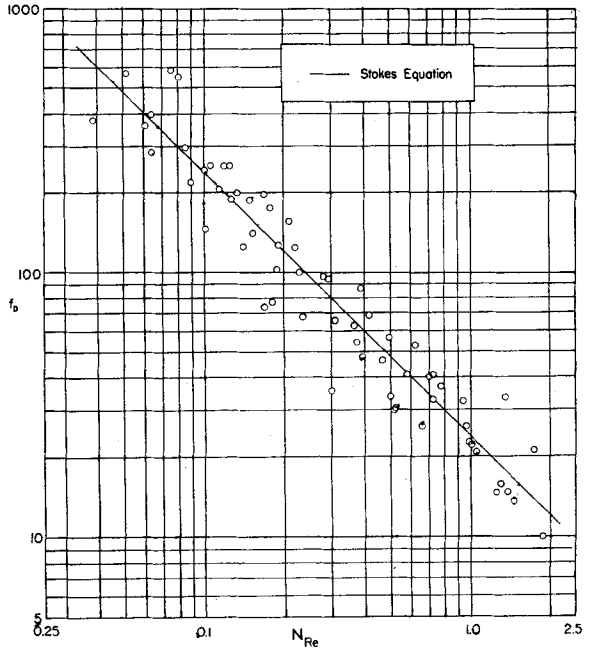

Fig. 3. Data for spheres.

$$\left[1 - \frac{1}{S}\left(S^2 - \frac{S}{2} + \frac{5}{16}\right)\frac{N_{Re}^2}{32}\right] \qquad (9)$$

$$S = 2.0022 - \ln N_{Re}$$

Tomotika and Aoi's solution for circular cylinders is in agreement with those of Bairstow, Cave, and Lang (2). Finn (3) measured the drag of an infinite cylinder immersed in a fluid at Reynolds numbers from 0.05 to 5.0 and obtained agreement with Equation (9) up to Reynolds numbers of 0.5. Wieselsberger (*17*) studied the Reynolds number range from 5 to 70, and his experimental drag coefficients were somewhat below predictions of Tomotika and Aoi. In the Reynolds number range from 5 to 10 the relaxation solution of Allen and Southwell (*1*) agrees with experimental data.

Imai (*5*) also presented a numerical solution to flow past an inclined elliptic cylinder for Reynolds numbers of 0.1 and 1.0. For circular cylinders Imai's results agree with those of Tomotika and Aoi.

Finn (3) found that when the fluid was not infinite the presence of the container walls had a considerable effect on the drag, particularly at low Reynolds numbers. For cylinders a distance of at least 500 diam. was necessary before wall effect became negligible. White (*16*) derived the following relationship showing the magnitude of this wall effect for an infinite cylinder between two parallel walls spaced a distance D_T apart:

$$f_D = C_w/N_{Re} \qquad (10)$$

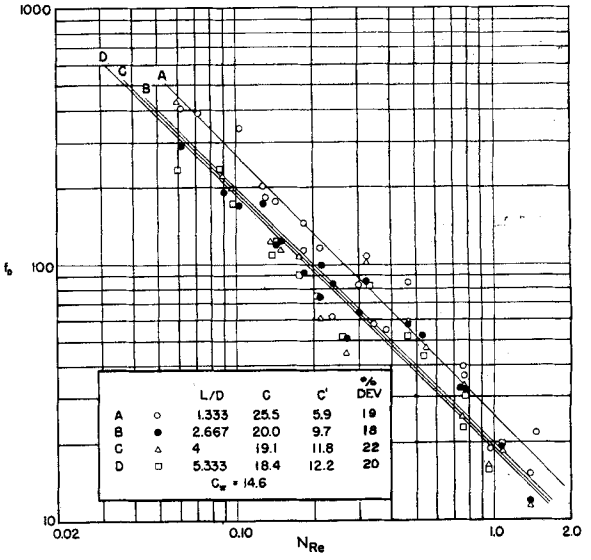

Fig. 4. Data for cylinders, $D_T/D = 9.17$.

where

$$C_w = \frac{12.6}{\log(0.8\,D_T/D)}$$

When the cylinder is of finite length, White proposed the end-effect correction to be added to C_w in Equation (10) as follows:

$$C_E = 20\left(\frac{D}{L}\right)\left(1 + 2.4\frac{D}{D_T - L}\right) \qquad (11)$$

Solutions for drag coefficients parallel to flat plates based upon Oseen's equations have been presented by Tomotika and Aoi (*15*), Tomotika and Yosinobu (*14*), and Piercy and Winney (*12*), all of whom present similar solutions.

Janssen (*7*) used an analogue computer to determine drag coefficients for flow parallel to flat plates at low Reynolds numbers. He obtained results substantially in agreement with experimental work of Janour (*6*), which extended down to a Reynolds number of 10. For Reynolds numbers below this Janssen's results agree with those of Tomotika and Aoi.

Analytical studies on the drag of infinite flat plates perpendicular to the flowing stream at low Reynolds numbers have been made by Imai (*5*) and Tomotika and Aoi (*14*). The results of these two investigations agree.

The experimental results obtained in the present study are compared with the analytical work described above.

EXPERIMENTAL EQUIPMENT

Force Measuring Equipment

The force measuring equipment was arranged as shown in the diagram in Figure 1.

The apparatus was constructed to move various bodies vertically through a viscous fluid. It consisted of a 1/6-hp. motor coupled to a speed reducer. A four-step V-pulley with diameters of ¾, 1¼, 1¾, and 2¼ in. was installed on the speed reducer. The drag force was measured by means of a 2-lb. spring scale with ½-ounce divisions. This scale was calibrated on a platform scale measuring to the nearest 0.001 lb. It was connected to the four-step pulley by means of a nylon cord. A capstan arrangement with a single turn around the pulley was used to connect the scale to the pulley. A weight was placed at the end of the cord, as shown in Figure 1. Several different weights were used in order to counterbalance the weights of the cylinders and spheres. With this arrangement a wider range of velocities was obtained.

A fine wire 0.003-in. diameter was used to connect the plates, cylinders, and spheres to the scale.

The fluid through which the objects were moved was contained in a 13.8-in. diameter, 15-gal. oil drum placed inside a 31-gal. drum. The inner drum rested upon a bracket inside the outer barrel, and cooling water was circulated through the annular space to maintain constant fluid temperature at 62° to 63°F.

Drag-force measurements were made on each body in two types of heavy duty gear oil. The relationship between temperature and viscosity was determined for each oil.

TABLE 1. SUMMARY OF BODIES STUDIED

Steel spheres

No.	Diameter, in.
1	¾
2	1
3	1½
4	2

Cylinders

No.	Length, in.	Diameter, in.
1-S*	2	¼
2-S	2	½
3-S	2	1
4-A*	2	1½
5-S	4	¼
6-S	4	½
7-S	4	1
8-A	4	1½
9-S	6	¼
10-S	6	½
11-S	6	1
12-A	6	1½
13-S	8	¼
14-S	8	½
15-S	8	1
16-A	8	1½

Flat plate—perpendicular flow

No.	Length of longest side, in.	Length of shortest side, in.	Thickness, in.
1-A	8	2	7/64
2-A	6	1 1/2	7/64
3-S	4	1	3/64
4-S	2	1/2	3/64
5-A	8	4	7/64
6-S	6	3	3/64
7-S	4	2	3/64
8-S	2	1	3/64
9-S	4	4	3/64
10-S	3	3	3/64
11-S	2	2	3/64
12-S	1	1	3/64

Flat plate—parallel flow (Steel, 3/64 in. thick)

No.	Length perpendicular to flow, in.	Length parallel to flow, in.	Thickness, in.
1a	4	1	3/64
1b	1	4	3/64
2a	4	2	3/64
2b	2	4	3/64
3	4	4	3/64
4a	4	8	3/64
4b	8	4	3/64

* S – Steel.
* A – Aluminum.

Bodies Studied

Measurements were obtained on the bodies described in Table 1. Small holes were drilled in the sphere and the ends of the cylinders, and ordinary cement was used to connect the 0.003-in. diameter wire to them. Small holes were drilled in the corner of the plates in order to attach the wires to them.

Procedure

A calibrated hydrometer was used to measure the density of the fluids used, and a viscometer was used to measure the viscosity of the fluids used. In addition the viscosity of the light oil was checked by means of the falling ball method.

The velocity of movement of the immersed bodies through the oil was measured by determining the rate of rotation of the pulleys. The error in the velocity was considered to be less than 0.5%.

In measuring the drag force on an object the object was connected to the spring scale and dropped to the bottom of the oil drum. The motor was started, and the scale was read as the object was being pulled toward the top of the drum. Two or three readings were taken for each body at each velocity. Of all the experimental measurements the largest error occurred in the force measurements. The force could be read to ± 1/6 of an ounce, and since some forces were of the order of 1 ounce, the possible error in the force measurement approached 20%. Most of the data were obtained at a temperature of 62° to 63°F.

EXPERIMENTAL DATA

Because of the large error in the force measurement there was considerable scatter of the data. A number of velocities were investigated for each body, and sufficient data were obtained so that a least-squares analysis of the results was possible. Detailed experimental data are available (*8*).

The equipment was first calibrated by measuring the drag on spheres of various diameters. It was found that the drag force of the wires attached to the bodies constituted a significant portion of the measured total drag force. The data on spheres were used to establish a relationship between the drag on the wire and the velocity. The wire drag was determined by applying Stokes' equation [Equation (3)] to calculate the drag force actually due to the sphere. This drag force was subtracted from the total measured drag force, the difference being due to the drag of the wire. The correction curves relating the drag force on the wire to the axial velocity of the wire are shown in Figure 2. These corrections apply for one wire, and when more than one wire is used the total correction is obtained by multiplying the correction by the number of wires that are attached to the immersed body.

The drag force shown in Figure 2 is that for a wire 0.003 in. in diameter moving axially out of the oil. This force

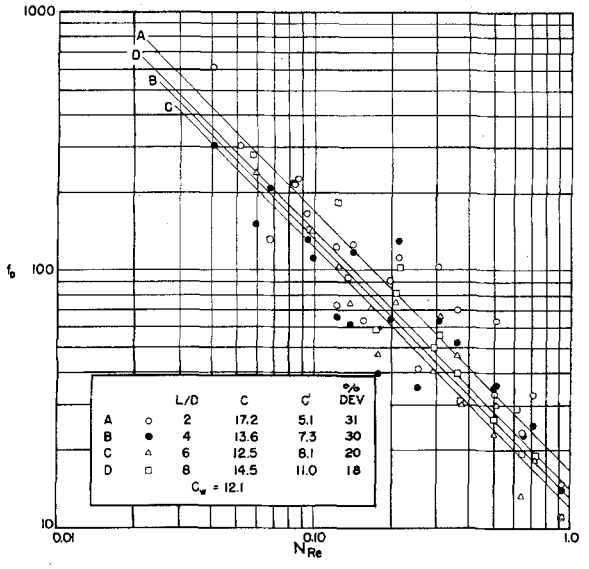

Fig. 5. Data for cylinders, $D_T/D = 13.75$.

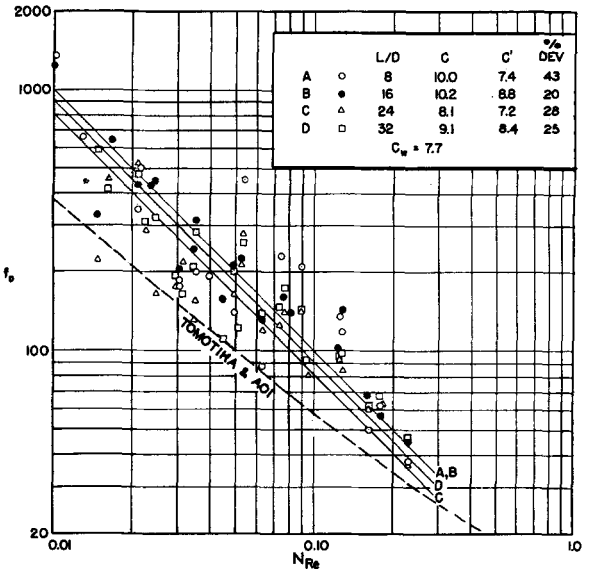

Fig. 7. Data for cylinders, $D_T/D = 55.0$.

is approximately proportional to the velocity. Actually the viscous drag force exerted on the wire will decrease as the wire is drawn out of the fluid. However a considerable amount of the oil adhered to the wire as it emerged from the fluid, and this added weight of oil was also detected by the spring scale. Therefore the force shown in Figure 2 is made up of two parts, the drag force due to the wire moving through the fluid and the force due to the weight of oil adhering to the wire. It appears that for a given velocity the drag force decreases at the same rate that the weight of oil on the wire increases, and therefore the force exerted by the wire itself remains relatively constant throughout the range of movement of the wire.

There was considerable scattering of the data, particularly in cases where the drag force was very low, and relatively large percentage of errors in reading the force on the spring scale occurred. In some instances the measured drag force was less than the correction applied for the drag force of the wires. A number of other points appeared to be extraordinarily far away from the main body of the data and were subsequently discarded in the analysis. Approximately 5% of all data points were discarded for these reasons.

In the flow range studied all data were analyzed by a least-squares method, with the assumption that the following equation could be used to represent the data:

$$f_D = C/N_{Re} \qquad (12)$$

Values of the coefficient C were determined for each body investigated.

EXPERIMENTAL RESULTS

Figure 3 shows the data obtained on all spheres after the correction shown in Figure 2 had been applied. The line represents Equation (3) and the data have an average deviation of 16% from the equation.

The data on the drag coefficients for cylinders are shown in Figures 4, 5, 6, and 7. In these figures the drag coefficient is plotted vs. the Reynolds number at a constant value of the ratio D_T/D (tank diameter/cylinder diameter). At the relatively low values of D_T/D encountered in this investigation it was found that the tank diameter did have considerable effect on the drag coefficient of the cylinders.

A summary of the experimental results on circular cylinders is tabulated on each of the figures showing values of C in Equation (12) and of C_w calculated from Equation (10). The coefficient C' shown in the tables is obtained by subtracting the end effect from C; that is

$$C' = C - 20\left(\frac{D}{L}\right)\left(1 + 2.4\frac{D}{D_T - L}\right) \qquad (13)$$

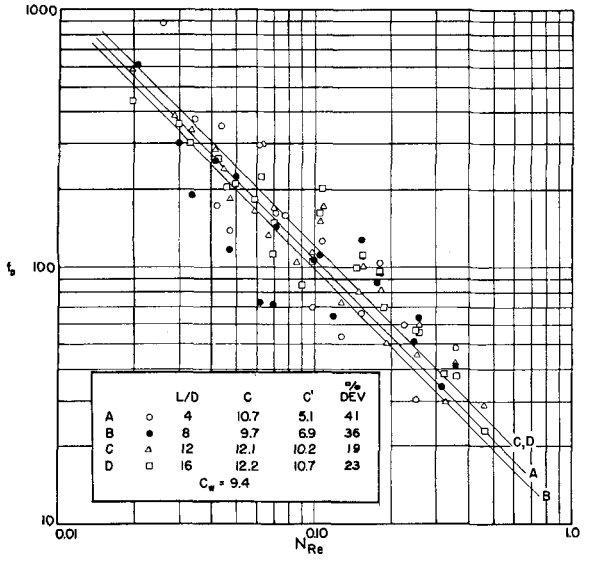

Fig. 6. Data for cylinders, $D_T/D = 27.5$.

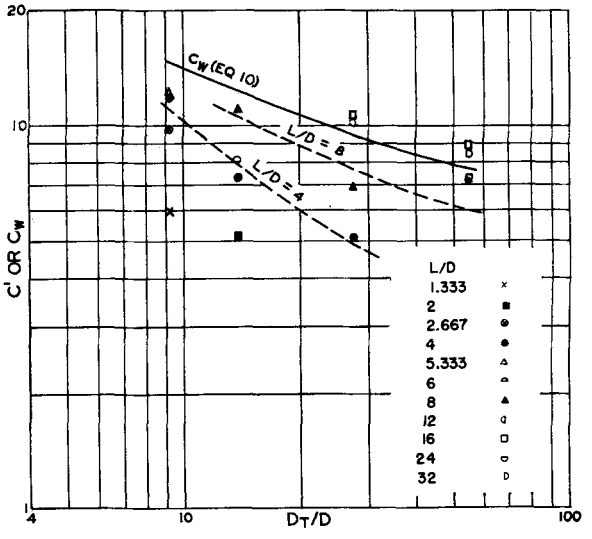

Fig. 8. Summary data on circular cylinders.

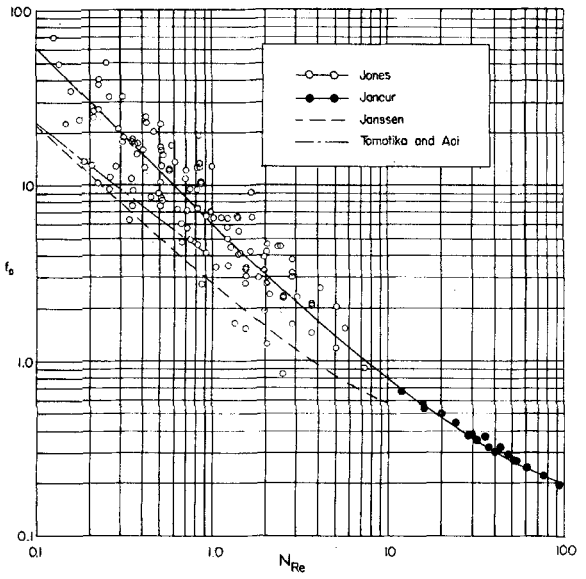

Fig 9. Data for flat plates in parallel flow.

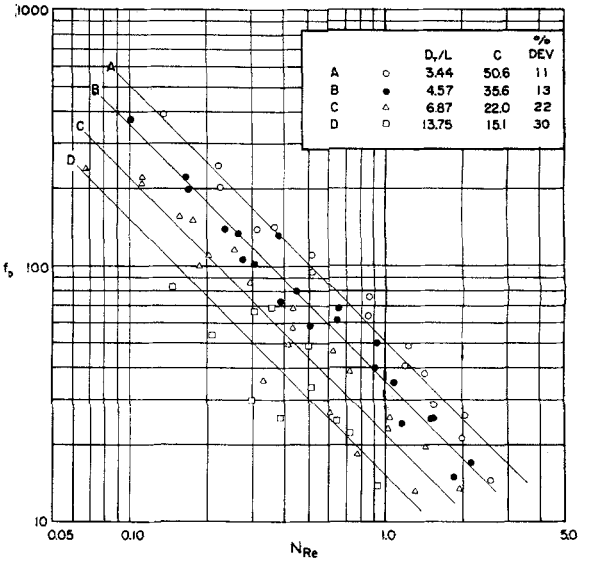

Fig. 11. Data for flat plates, $W/L = 2$.

Average per cent deviations of the data from Equation (12) are also shown on the figures. This average deviation ranged between 18 and 43%, with most of the groups of data having a deviation between 20 and 30%. This deviation is brought about largely by the error in the force measurement.

The results of the investigation on circular cylinders are summarized in Figure 8, in which C' and C_w are plotted vs. the ratio D_T/D. The upper curve in Figure 8 is a plot of C_w as calculated from Equation (10). It is noted that at low L/D ratios the value of C' is much less than C_w. The curves for C' at $L/D = 4$ and $L/D = 8$ are shown and lie below the curve given by Equation (10). As the L/D ratio becomes greater than 16, the values of C_w and C' approach each other.

It is concluded from these results that White's equations [Equations (10), (11)] may be used to predict drag coefficients for circular cylinders moving in tanks of finite diameter (in the D_T/D range studied) if the L/D ratio of the cylinder is greater than 16. For L/D ratios less than 16 the lower curves shown in Figure 8 may be used to predict the drag coefficients for such cylinders.

The analytical results of Tomotika and Aoi for infinite cylinders in an infinite fluid are plotted in Figure 7. Their results are in reasonably good agreement with those obtained on circular cylinders having L/D ratios of 24 and 32 for the case when the ratio D_T/D is equal to 55.0. These experimental conditions approximate the conditions applicable to the analytical solution of these workers.

Figure 9 shows all of the data obtained on flat plates in parallel flow. The analytical results of Janssen (7), Tomotika and Aoi (15), and the experimental values of Janour (6) are shown. Up to a Reynolds number of 2 the least-squares line through the present data has the following equation:

$$f_D = 5.91/N_{Re} \qquad (14)$$

The drag coefficients on flat plates in parallel flow were obtained on plates of finite size, and therefore an edge correction had to be applied. The edge correction used was that recommended by Janour:

$$F_{edge} = 1.6\,\mu\,LU/g_c \qquad (15)$$

Equation (15) represents the forces due to one edge of the flat plate in parallel flow. The empirical equation obtained in the present work when extrapolated fits Janour's experimental data quite well. However it lies considerably above analytical results.

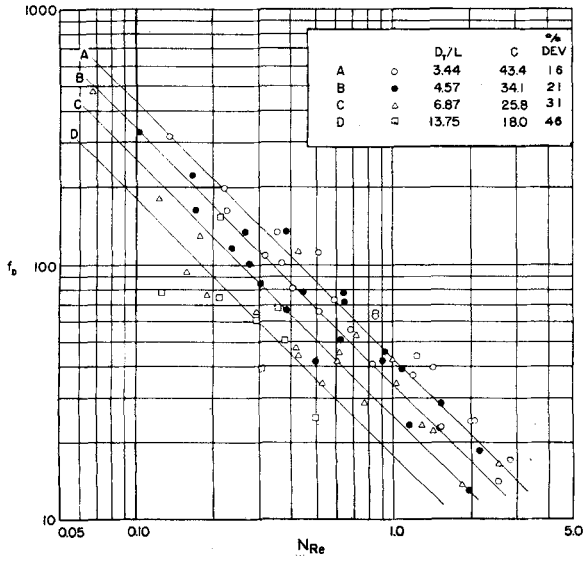

Fig. 10. Data for flat plates, $W/L = 1$.

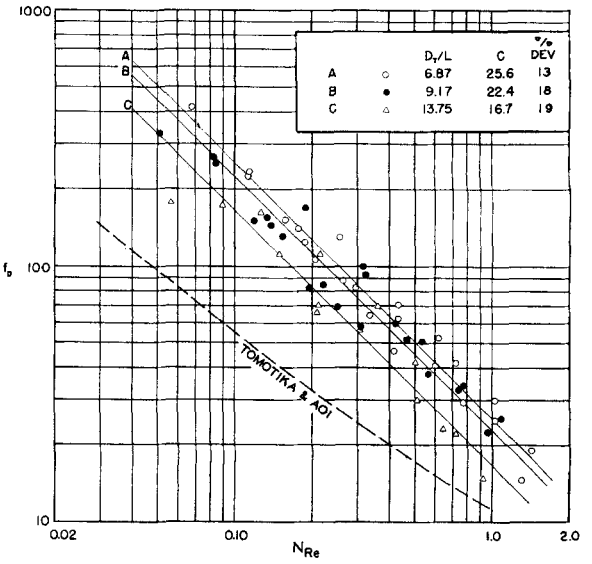

Fig. 12. Data for flat plates, $W/L = 4$.

The data for flat plates in perpendicular flow are shown in Figures 10, 11, and 12, where the drag coefficient is plotted vs. the Reynolds number at constant values of the ratio W/L, which is the ratio of the length of the long side of the flat plate to the length of the short side. In each figure a definite effect of the ratio D_T/L is indicated. The data for all flat plates in perpendicular flow are summarized on the figures, and the average deviation from Equation (10) ranges between 11 and 46%, with most of it lying between 11 and 22%. It is probable that smaller errors occurred for the measurements with plates in perpendicular flow, since the drag forces for these bodies were much higher than for the other bodies tested.

In Figure 13 the value of C is plotted vs. the ratio D_T/L for all flat plates in perpendicular flow. In the range $1 < W/L < 4$ no significant effect of W/L on the value of C could be detected. Therefore the curve shown in Figure 13 is recommended for determining values of the drag coefficient for flat plates in perpendicular flow in the ranges $1 < W/L < 4$ and $3 < D_T/L < 14$.

CONCLUSIONS

Drag coefficients at low Reynolds numbers have been determined for flow past spheres, circular cylinders, and flat plates, both parallel and perpendicular to the flow. Experiments were carried out with two grades of heavy duty gear oil and by determining the force required to pull the body through the oil at a given velocity. With Stokes' equation used as a basis the data for spheres were used to determine correction factors for the drag forces on the wires that were attached to the immersed bodies. In all cases at low Reynolds numbers the drag coefficient appeared to be inversely proportional to the Reynolds number, and a least-squares analysis of the data was used to determine the value of C in the equation

$$f_D = C/N_{Re} \qquad (12)$$

In the range of D_T/D studied the equations [Equations (10), (11)] recommended by White (*16*) involving the wall effect and end correction agree with the experimental data for values of L/D greater than 16. At L/D ratios less than 16 drag coefficients are lower than those predicted from White's equations, and the experimental curves for L/D ratios of 4 and 8 may be used to predict drag coefficients for this type of cylinder.

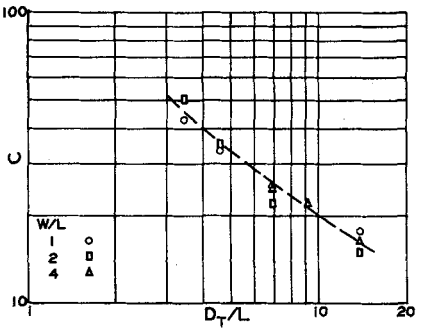

Fig. 13. Effect of tank diameter on drag coefficients of flat plates in perpendicular flow.

For flat plates of infinite span in parallel flow the following equation was obtained:

$$f_D = 5.91/N_{Re} \qquad (14)$$

$$0.01 \leq Re \leq 2.0$$

[For finite plates an edge correction given by Equation (15) must be added to the drag force calculated from Equation (14)].

For flat plates in perpendicular flow no effect of W/L ratio was detected in the range investigated in this work. The tank diameter however had considerable effect on the drag coefficients of flat plates in perpendicular flow, and the curve in Figure 13 may be used to predict drag coefficients for flat plates in perpendicular flow within the ranges of D_T/L and W/L indicated on the figure.

ACKNOWLEDGMENT

The authors wish to take this opportunity to extend appreciation to the Dow Chemical Company for a graduate fellowship, under which this research was carried out.

NOTATION

A_p = projected area of cylinders, spheres, or plates in perpendicular flow; wetted area of flat plate in parallel flow, sq. ft.

C = coefficient appearing in Equation (15)

C' = $C - C_E$

C_E = end-effect correction

C_w = coefficient appearing in Equation (13)

D = cylinder or sphere diameter, ft.

D_T = tank diameter; spacing between parallel planes, ft.

F = drag force, lb.$_f$

F_{edge} = drag force due to edge of flat plate, lb.$_f$

f_D = drag coefficient defined by Equation (1)

g_c = gravitational constant, 32.17 lb.$_m$ ft./lb.$_f$ sec.^{2}

L = length of short side of plate in perpendicular flow; length of flat plate parallel to direction of flow in parallel flow; length of cylinder, ft.

N_{Re} = Reynolds number, DU/ν for cylinders and spheres, LU/ν for flat plates

r = radius, ft.

S = factor in Equations (10), (11), and (12)

t = time, sec.

U = velocity of undisturbed stream or velocity of immersed body through fluid, ft./sec.

W = length of long side of flat plate in perpendicular flow, span of flat plate in parallel flow

μ = viscosity, lb.$_m$/ft. sec.

ν = kinematic viscosity, sq. ft./sec.

ρ = density, lb.$_m$/cu. ft.

LITERATURE CITED

1. Allen, D. N. de C., and R. V. Southwell, *Quart. J. Mech. Appl. Math.*, **8**, 129 (1955).
2. Bairstow, L., B. M. Cave, and E. D. Lang, *Phil. Trans. Roy. Soc. London*, **A233**, 383 (1923).
3. Finn, R. K., *J. Appl. Phys.*, **24**, 771 (1953).
4. Goldstein, Sidney, *Proc. Roy. Soc. London*, **A123**, 225 (1929).
5. Imai, I., *ibid.*, **A224**, 141 (1954).
6. Janour, Zbynek, *Natl. Advisory Comm. Aeronaut., Tech. Memo. 1316* (November, 1951).
7. Janssen, E., 1956 Heat Transfer and Fluid Mechanics Institute, Preprint of papers, p. 173, Stanford Univ. Press, California (1956).
8. Jones, A. M., M.S. thesis, Oregon State College, Corvallis (June, 1958).
9. Lamb, Horace, *Phil. Mag. J. Sci.*, **6**, No. 21, 112 (1911).
10. Liebster, H., *Ann. Physik*, **4**, No. 82 341 (1927).
11. Oseen, C. W., *Arkiv. Mat. Astron. Fysik*, **6**, 75 (1910); **9** (1913).
12. Piercy, N. A. V., and H. F. Winney, *Proc. Roy. Soc. London*, **140A**, 543 (1953).
13. Stokes, George Gabriel, "Mathematical and Physical Papers," Vol. 3, Cambridge Univ. Press (1922).
14. Tomotika, S., and H. Yosinobu, *J. Math. Phys.*, **35**, 1 (1956).
15. Tomotika, S., and T. Aoi, *Quart. J. Mech. Appl. Math.*, **6**, 290 (1953).
16. White, C. M., *Proc. Roy. Soc. London*, **186A**, 472 (1946).
17. Wieselsberger, C., "Ergebnisse der Aerodynamischen Versuchsanstalt," Vol. 2 (1923).

Manuscript received February 5, 1959; revision received May 2, 1960; paper accepted May 3, 1960.